Influence of the storage period between charge and discharge in a latent heat thermal energy storage system working under partial load operating conditions

Jaume Gasia[1], Alvaro de Gracia[1,2], Gabriel Zsembinszki[1], Luisa F. Cabeza[1,*]

[1]GREiA Research Group, INSPIRES Research Centre, Universitat de Lleida, Pere de Cabrera s/n, 25001-Lleida, Spain

[2]CIRIAF – Interuniversity Research Centre on Pollution and Environment "Mauro Felli", Via Duranti 63, 06125-Perugia, Italy

*Corresponding author: Tel: +34.973.00.35.76. Email: lcabeza@diei.udl.cat

Abstract

The supply intermittency of energy sources like solar energy or industrial waste heat should be properly addressed when studying latent heat thermal energy storage (TES) systems, since it might cause an incomplete melting/solidification of phase change materials (PCM). In the present paper, and experimental study was performed to analyse the storage period (also known as stand-by period) in a latent heat TES system working under partial load operating conditions and the effect of its duration on the subsequent discharging process. In the experimental set-up, 99.5 kg of high density polyethylene (HDPE) was used as PCM in a 0.154 m^3 storage tank based on the shell-and-tube heat exchanger concept. Four different percentages of charge were evaluated: 58%, 73%, 83% (partial charge), and 97% (full charge). Each charging level was followed by three different periods of storage: 25 min, 60 min, and 120 min. The fact of working at different levels of charge caused that in some regions of the TES system the PCM was not completely melted. Thus, at the end of the charging process different levels of thermal homogenisation were observed. However, during the storage period, the PCM temperature showed a tendency to homogenisation, which was influenced by the energy distribution within the PCM, the heat losses, and the duration of the storage period. Focusing on the discharging period, it was observed that the duration of the storage period slightly affected the temperature and heat transfer profiles, causing the main differences of performance during the first 30 min of process.

Keywords: Thermal energy storage; Phase change material; Partial loads; Incomplete melting; Storage period; Stand-by period.

Nomenclature

Cp	Specific heat, J/kg·K
E	Energy, J or kWh
h	Enthalpy, J/kg or kWh/kg
m	Mass, kg
$\dot{m}$	Mass flow rate, kg/s
R	Function that depends on the measured parameters
t	Time, s
T	Temperature, ºC
V	Volume, m^3
w	Uncertainties associated to the independent parameters
W	Estimated uncertainty in the final result
x	Independent measured variables
ρ	Density, kg/m^3
λ	Thermal conductivity, W/m·K

Subscripts

c	Corner
ch	Charge
dch	Discharge
fs	Final time of the storage process
i	Instant
in	Central part of the storage tank when it refers to the PCM
	Inlet of the storage tank when it refers to the HTF
is	Initial time of the storage process
ins	Insulation
loss	Losses
m	Melting
n	Control volume
out	Outlet of the storage tank
pr	Process
s	Solidification
st	Storage
tank	Metal parts of the storage tank
sub	Subcooling

Abbreviations

DSC	Differential scanning calorimeter
HDPE	High density polyethylene
HTF	Heat transfer fluid
HTR	Heat transfer rate
MF	Melt fraction
PCM	Phase change material
RAE	Ratio of accumulated energy
TES	Thermal energy storage

1 Introduction

Reducing greenhouse gases emissions and therefore, fighting against climate change, which is responsible of several catastrophes around the world, implies shifting towards a more sustainable society. This means that households, industries, governments, etc. must find an equilibrium between economic prosperity, technological competitiveness, and environment benefits. Two of the easiest actions which can be carried out to achieve such equilibrium are the deployment of renewable energies and the reuse of wastes. From the thermal energy point of view, the main targets for this deployment are solar energy and industrial waste heat (IWH) use, due to their high availability and energy potential [1,2]. However, they have a major drawback which limits their harnessing, the intermittency in their thermal energy supply. As a consequence, mismatches between energy supply and demand might occur and therefore, the thermal process associated to them might be forced to work under partial load operating conditions.

Thermal energy storage (TES) is a key technology that can address the intermittency of both solar energy and IWH and thus, helping to the reliability of the system. Moreover, TES allows increasing the facility generation capacity by taking advantage of the thermal energy excess during low-demand periods, and increasing the versatility of the system by levelling peak load demand periods and achieving off-peak consumption [3]. The basic principle of TES is the storage of energy from a heat supply to be further used by a heat sink, usually through an intermediate heat transfer fluid (HTF). A full TES cycle involves the processes of charge, storage, and discharge. Thus, the heat obtained from the TES system during the discharging process not only depends on how the energy was supplied into the system during the charging process, but also depends on the behaviour of the TES system during the storage process. Among the different TES technologies, latent heat TES is considered one of the most promising due to its high energy density [4]. For example, during the phase change of 1 kg of ice, about 334 kJ of energy can be stored. On the contrary, if the same amount of energy is required to be stored in the sensible form, the water storage system would require a temperature gradient of 79 ºC, which can cause problems with heat losses, stratification control, etc. [5]. Several studies were carried out in order to optimize and maximize the operation of latent heat TES systems, focusing on evaluating the influence of the HTF mass flow rate, HTF inlet temperature, PCM melting temperature, number of PCM in multiple PCM configurations, PCM effective thermal conductivity, TES system dimension, sensible heating, and subcooling [6]. However, the gross majority of those studies did not take into account two important considerations. On one hand, the storage period between the charging and discharging processes, since these studies are mainly focused on the charge and discharge, either as separate processes or as continuous

processes [7,8]. On the other hand, working under partial load operating conditions, which might lead the PCM to be partially charged/discharged and, as a consequence, to not fully undergo phase change [9]. Thus, the aim of this paper is to study if the variation of the duration of the storage period (also known as stand-by period) in a latent heat TES system which has been previously partially or totally charged has any influence on the subsequent discharging process.

For the storage process it is important to be properly evaluated since the thermal distribution at the end of the preceding process (either charge or discharge) may be different than the thermal distribution at the beginning of the subsequent process, especially in partially charged/discharged latent TES systems. To the best of the authors knowledge, only four studies did an attempt to evaluate the storage process after interrupting a charging/discharging process. Toksoy and Ilken [10] observed, with a mathematical model, that in a storage process which followed an interrupted freezing process, the phase change process continued until the temperature distribution in the whole system became uniform. Similarly, Bejarano et al. [11] performed a series of partial charging/discharging operations with a short storage period. Results showed that during the storage period the PCM continued storing/releasing energy because of the thermal inertia of the intermediate fluid. Hence, it is important that both, the temperature distribution due to the temperature gradient within the TES material and the heat losses to the surroundings, are properly taken into account during the storage period. Following this idea, Jegadheeswaran et al. [12] stated that the storage period required in a TES system has a high influence on its final thermo-economic analysis results. Another study carried out by Hirano [13] evaluated the behaviour of a latent heat TES system, after being fully charged, under three different storage periods (36 h, 7 days, and 2 months). They observed that after two-month-period storage, about 40% of the input energy was lost and 10% of it was due to the cooling operation for nucleation. Moreover, they observed that the temperature of the storage tank showed a tendency to homogenise to the ambient temperature, as a result of the heat losses. It has to be mentioned that most of the research which studied the temperature distribution and heat losses within a TES system were mainly focused on sensible TES materials, such as packed beds [14], water [15] or molten salts [17].

As mentioned above, partial load operating conditions are very likely to happen in real thermal processes where PCMs are used and, therefore, incomplete melting and/or freezing cases may still occur. This is even more sensitive in PCM which present specific effects such as hysteresis and/or subcooling [17,18]. There is currently no consensus on how to address in numerical models the transition between heating and cooling in TES systems working under partial load operating conditions from the enthalpy-temperature curve point of view. Four different

methodologies are currently available in the literature defining how to model such transition in a partially melted/solidified PCM [19-22], highlighting the need for experimental studies which shed light on the matter and define the proper methodology of modelling. The first [19] and second [20] methodologies state that one can change from one curve to the other. The only difference is the slope of the change, either parallel to the curve in the sensible region [19] or without [20]. The third methodology [21] suggests to remain in the same curve. Finally, the fourth methodology [22] states that the curve is placed between the cooling and heating curves. Differential scanning calorimeter (DSC) analyses carried out by Li et al. [23] showed that the peak in melting process gradually decreased in incomplete phase change processes, and that the relationship of heat flow with temperature also showed a different behaviour. Bedecarrats et al. [24] and Avignon and Kummert [25] experimentally observed that interrupting heating/cooling processes before the PCM was completely melted or solidified also had an effect on the phase change temperature and on the degree of subcooling. Palomba et al. [26] noticed that the level of charge, or discharge, in incomplete phase change processes influenced their subsequent processes. Finally, in a previous study carried out by Gasia et al. [27], five percentage of charge (58%, 73%, 83%, 92%, and 97%) and their influence on the discharging process were evaluated in a latent heat TES system. Results from the experimentation showed that partially charging the TES system above 85% of its maximum energy capacity becomes a good option if the final application accepts a maximum decrease of discharging heat transfer rates of 10% if compared to the fully charged system.

From the literature review, it is observed that there is still a lack of experimental results which evaluate the effect of the storage period duration in cyclic processes working under partial load operating conditions. Therefore, continuing the previous work [27], this paper analyses the influence that the duration of different storage periods (25 min, 60 min, and 120 min) after partially charged (charging levels of 58%, 73%, and 83%) and fully charged processes has on the same storage periods and on their subsequent discharging processes.

2 Materials and method

2.1 Materials

High density polyethylene (HDPE) was the PCM used in this experimentation. Table 1 and Figure 1 summarize the main thermophysical properties of HDPE. Moreover, pilot plant analyses carried out in a previous study by Gasia et al. [27] showed that the melting process occurred between 127 °C and 136 °C and that the solidification occurred between 127 ºC and 124 ºC [27], in accordance to what it was observed in Rathgeber et al. [31].

Table 1. Summary of the main thermo-physical properties of HDPE.

Parameter		Value		Ref.
Melting temperature	T_m	124 – 134 ºC		[27]
Solidification temperature	T_s	126 – 124 ºC		[27]
Melting enthalpy	ΔH_m	137.8 kJ/kg		[27]
Solidification enthalpy	ΔH_s	130.7 kJ/kg		[27]
Specific heat	Cp	@100 ºC	2.4 – 2.8 kJ/kg·K	[27-29]
		@150 ºC	2.3 – 2.7 kJ/kg·K	[27-29]
Density	ρ	@100 ºC	990 kg/m^3	[30]
		@150 ºC	786 kg/m^3	[27]
Thermal conductivity	λ	@100 ºC	0.35 – 0.38 W/m·K	[28,29]
		@150 ºC	0.19 W/m·K	[28]
Subcooling	ΔT_{sub}	No subcooling was detected		[27]

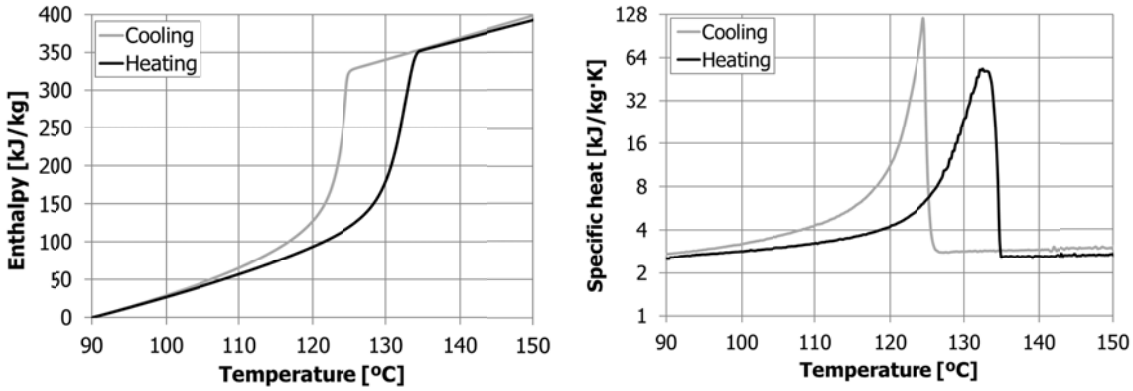

Figure 1. High density polyethylene enthalpy-temperature (a) and specific heat-temperature curves (b) [27].

2.2 Experimental set-up

This study was performed at the pilot plant facility available at the University of Lleida, whose high versatility allows testing and characterizing sensible and latent heat TES systems up to 400 ºC [27,32]. The storage system was a 0.154 m^3 tank based on the shell-and-tube exchanger concept (Figure 2a) whose lateral walls and cover were insulated with 240 mm of rock wool (90.4 kg) and whose bottom region was insulated with 450 mm of foam glass (91.4 kg). It contained 99.5 kg of HDPE distributed within the tank in three representative regions as shown in Figure 2b: 79% of the PCM was placed around the tubes bundle (main part), 14% of the PCM

was placed in the region between the tubes bundle (central part), and the remaining 7% was located in the corners. With the aim of monitoring the behaviour of the latent heat system several Pt-100 1/5 DIN class B temperature sensors were installed. Thirty-one of them were installed in the three representative regions of the storage tank (Figure 2c and Figure 2d). Each sensor was associated to a PCM control volume, which allowed a better monitoring and analysis of the PCM behaviour. Two temperature sensors were located at the inlet and outlet of the HTF tubes bundle to measure the HTF temperature (Figure 2d). Finally, six temperature sensors were placed on the walls of the storage tank and on the walls of the insulation to evaluate the energy accumulated by the tank and by the insulation, as well as to evaluate the heat losses to the surroundings.

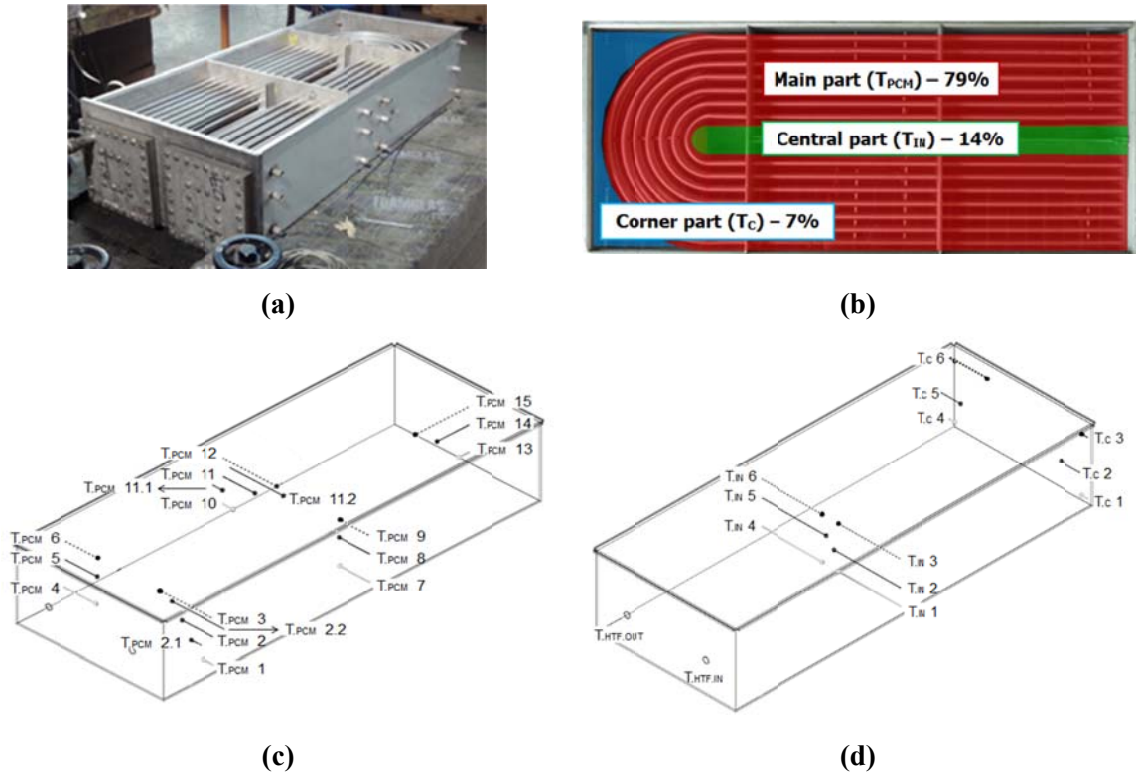

Figure 2. TES system used in the experimental setup: (a) Overview of the TES system; (b) PCM distribution within the TES system; (c) PCM temperature sensors of the main part; (d) Inlet and outlet HTF temperature sensors, and PCM temperature sensors of the corner and central parts [27].

2.3 Methodology

The experimentation consisted of twelve complete cycles (Table 2). These cycles presented three stages, as shown in Figure 3. The first stage was the charging process. In this stage, the PCM was initially at a homogeneous average temperature of 105 ± 1 ºC and the HTF entered the TES system at a temperature of 155 ± 2 ºC and a mass flow rate of 0.5 ± 0.01 kg/s. Four

different charging levels were evaluated, following the previous study carried out by Gasia et al. [27]. Hence, the charging processes were stopped after a period of time (Δt_{CH}) which depended on the ratio of accumulated energy (RAE). This performance indicator defines the amount of energy accumulated in the PCM at a certain time interval in front of the theoretical maximum energy that can be stored by the PCM if fully charged. Therefore, the charging time was: 41 ± 1 min (RAE 58%), 70 ± 1 min (RAE 73%), 150 ± 1 min (RAE 83%), and 1440 ± 5 min (RAE 97%). These processes were followed by a storage period, in which no HTF recirculation within the storage tank took place. The duration of this period (Δt_{ST}) was a parameter defined by the authors of the current study. Three different storage periods were evaluated: 25 ± 1 min, 60 min ± 1 min, and 120 ± 1 min. Authors tried to represent potential storage periods in processes working under partial load operating conditions, such as industrial and solar processes, which might need the heat from the latent heat TES system even though they are not completely charged. It should also be mentioned that 25 min was the minimum storage period required to carry out the change from charge to discharge, and vice versa, since it is the minimum time needed by the experimental facility to achieve the set-point temperatures in each process. Finally, the third stage of the cycle was the discharging process, where the energy stored in the system is recovered by recirculating HTF at an average temperature of 105 ± 2 ºC and a mass flow rate of 0.5 ± 0.01 kg/s. In that case, the process was finished when the PCM reached steady conditions. Each of the twelve whole charging-storage-discharging cycle carried out in the present study was repeated three times to demonstrate repeatability of the methodology and the experimental results, ending up with the realization of thirty-six complete cycles.

Table 2. Set of experiments carried out in this study.

Experiment	**RAE**	**Δt_{ST}**		**Experiment**	**RAE**	**Δt_{ST}**
1	97%	25 ± 1 min		7	73%	25 ± 1 min
2	97%	60 ± 1 min		8	73%	60 ± 1 min
3	97%	120 ± 1min		9	73%	120 ± 1min
4	83%	25 ± 1 min		10	58%	25 ± 1 min
5	83%	60 ± 1 min		11	58%	60 ± 1 min
6	83%	120 ± 1min		12	58%	120 ± 1min

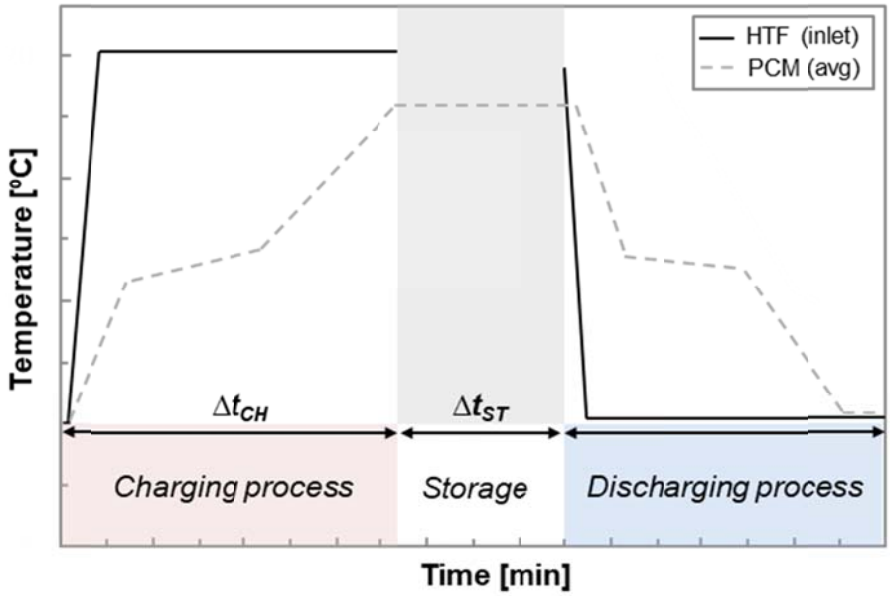

Figure 3. Stages of a complete charging/discharging cycle.

2.4 Theory and calculation

This section presents the equations used to obtain the results presented in the results and discussion section. The PCM weighted average temperature, according to the three representative regions of the storage tank (Figure 2b), was calculated as shown in Eq. 1:

$$T_{PCM.total,i} = \frac{\sum_{n=1}^{15} m_{PCM,n} \cdot T_{PCM,n,i} + \sum_{n=1}^{6} m_{in,n} \cdot T_{in,n,i} + \sum_{n=1}^{6} m_{c,n} \cdot T_{c,n,i}}{m_{PCM} + m_{in} + m_c} \quad (1)$$

The variations of the energy levels of PCM, HTF, metal parts of the storage tank, and insulation were calculated as given in Eq. 2, Eq. 3, Eq. 4, and Eq. 5, respectively:

$$\Delta E_{PCM.total} = \sum_{n=1}^{27} m_{PCM,n}\, \Delta h(T)_{n,fs-is} = \Delta E_{PCM.main} + \Delta E_{PCM.in} + \Delta E_{PCM.c} \quad (2)$$

$$\Delta E_{HTF} = \rho_{HTF} \cdot V_{HTF} \cdot Cp_{HTF} \cdot \Delta T_{HTF,fs-is} \quad (3)$$

$$\Delta E_{tank} = m_{tank} \cdot Cp_{tank} \cdot \Delta T_{tank,fs-is} \quad (4)$$

$$\Delta E_{ins} = m_{ins} \cdot Cp_{ins} \cdot \Delta T_{ins,fs-is} \quad (5)$$

Finally, the energy lost during the process was calculated through an energy balance, as shown in Eq. 6:

$$\Delta E_{loss} = -(\Delta E_{PCM.total} + \Delta E_{HTF} + \Delta E_{tank} + \Delta E_{ins}) \quad (6)$$

The HTF heat transfer rate at time "i" during the discharging processes that follows a storage period was calculated by means of Eq. 7:

$$\dot{Q}_{HTF,dch,i} = \dot{m}_{HTF,i} \cdot Cp_{HTF,i} \cdot \Delta T_{HTF,in-out,i} \quad (7)$$

2.5 Uncertainty analysis

An uncertainty analysis of the HTF heat transfer rate and the PCM accumulated energy of different charging and discharging processes was carried out in a previous study [27] to determine the precision and general validity of such results. In this paper, the uncertainty analysis is extended to include the storage period between a (partial) charge and the subsequent discharge of the latent heat TES system. Furthermore, the present analysis also includes an uncertainty analysis related to the energy variations in the HTF, the metal parts of the tank, the insulation, and the heat losses (for the storage period).

Two types of uncertainties may be distinguished in the analysis (Table 3): uncertainties associated to experimentation and uncertainties associated to the thermos-physical properties of the HTF, PCM, metal parts of the tank, and insulation.

Table 3. Uncertainties of the different parameters involved in the analyses.

Parameter	Units	Source	Accuracy
Temperature	ºC	Pt-100 1/5 DIN class B	± 0.2
HTF flow rate	l/h	FUJI FCX-A2 V5 series transmitter	± 23.7
HTF specific heat	kJ/kg·ºC	From ref. [33]	± 0.054
HTF density	kg/m^3	From ref. [33]	± 25.16
HTF volume	%	Estimated	± 3
PCM mass	kg	Regular scale	± 0.28
PCM volume	m^3	From manufacturer	± 0.0024
PCM enthalpy	kJ/kg	Sensors from Mettler Toledo DSC-822e	± 3
Insulation mass	%	From manufacturer	± 3
Insulation specific heat	%	From manufacturer	± 3
Metal parts volume	%	From manufacturer	± 3
Metal parts specific heat	%	From manufacturer	± 3
Metal parts density	%	From manufacturer	± 3

Next, the influence of these uncertainties on the results was determined by means of Eq. 8 [34]. All uncertainties were calculated for the storage period, except for the HTF heat transfer rate, which was calculated for the discharging process.

$$W_R = \left[\left(\frac{\partial R}{\partial x_1}\cdot w_{x_1}\right)^2 + \left(\frac{\partial R}{\partial x_2}\cdot w_{x_2}\right)^2 + \cdots + \left(\frac{\partial R}{\partial x_n}\cdot w_{x_n}\right)^2\right]^{1/2} \quad (8)$$

3 Results and discussion

3.1 Repeatability

Figure 4 shows the repeatability of different cycles for the cases with a storage period duration between charge and discharge of 60 min. Notice that only four cycles out of twelve are presented in this figure but it has to be mentioned that the remaining cycles also showed a similar tendency. On one hand, Figure 4a presents the evolution of the inlet HTF temperature during the charging (warm colours) and discharging processes (cold colours) for the four different RAE. In all cases the temperature follows practically the same trend with a delay of one to four minutes during the first 14 min of process (either charge or discharge) due to the differences in the stabilization process of the HTF temperature controller. At the moment the stationary regime was achieved, the temperatures followed the same profiles. On the other hand,

Figure 4b shows the evolution of the PCM temperature at control volumes evaluated by the temperatures sensors $T_{PCM.8}$ (straight line), $T_{IN.1}$ (dashed line), and $T_{C.6}$ (dotted line) during the charging process (as referred in Figure 2). The temperature profiles followed almost the same profile, with a deviation lower than 5% during the first 20 minutes and lower than 1% from that moment on. Thus, it can be concluded that the results presented in this work show repeatability.

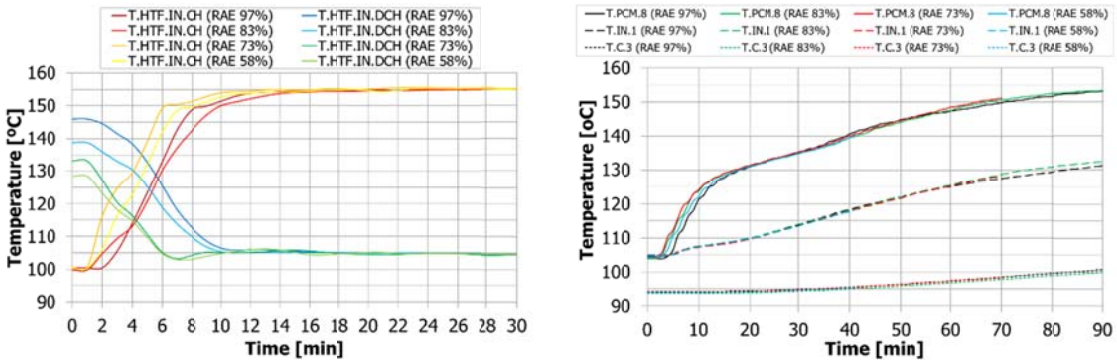

(a) **(b)**

Figure 4. Repeatability tests for the study when the duration of the storage period was 60 minutes. (a) HTF inlet temperatures during the charging and discharging processes; (b) PCM temperature at three different locations (evaluated by the temperature sensors $T_{PCM.8}$, $T_{IN.1}$, and $T_{C.3}$) during the charging process

3.2 Storage process

Figure 5 shows the PCM temperature evolution of different control volumes in the three main regions of the storage tank during a storage period of 120 min for the four different tested RAE. Notice that due to the repeatability of results shown in the previous section, the PCM temperature evolution during the storage periods of 25 and 60 min can be analysed in the same figure. Moreover, the variation of the PCM average temperature and energy accumulated in the different regions of the tank, as well as the energy variation in the metal parts of the storage tank and in the insulation, and the heat losses are summarized from Table 4 to Table 7. Each table shows the results for each of the four RAE evaluated during the charging process.

It can be observed that when the charging process was stopped at a RAE 58% (Figure 5a) and the storage period started, the temperature of the PCM inside the tank was not homogeneous. The PCM located in the main region (straight line) was at a higher temperature than the PCM located in the central region (dashed line) and corners (dotted line). Furthermore, within the same regions, differences can be observed. The reason lies on the low thermal conductivity of HDPE (<0.4 W/m·K at the temperature range evaluated [28]), the geometry of the storage tank, and the level of charge. However, as the storage period keeps going, two different phases can be

observed. On one hand, during the first 10 min there was an increasing of temperatures on practically all PCM control volumes because of the thermal inertia of the HTF and the metal parts of the storage tank. This turned out into an increase of the energy available to be transferred to the PCM, which was at a lower temperature. On the other hand, from that moment on, a clear tendency to homogenization of temperatures, and therefore of the energy level, was observed. Energy from the PCM located at the main region was transferred to the PCM located at the central region and corners but also to insulation and lost to the environment (Table 4). During 120 min of storage, the average temperature of the PCM located at the main region decreased 5.5 ºC, while the average temperature of the PCM located at the central region and corners increased 0.4 ºC and 9.1 ºC, respectively. Moreover, the PCM that was under phase change at beginning of the storage showed temperature variations within the melting temperature range during the storage process, indicating that the melting front suffered a modification during the process, whose extend could not be quantified because of the current set-up acquisition methodology.

For shorter periods of storage, a similar tendency was observed, being the variation of temperature and energy levels between the end of the charging process and the beginning of the discharging process smaller than the variation over the storage periods of 120 min. Focusing on the PCM distribution within the tank, it can be seen that the material located in the main region losses less energy to its surrounding, or even it is still absorbing energy at lower RAE, as a result of the above-mentioned influence of the thermal inertia of the HTF and the metal parts of the tank. This is translated to a less energy absorbed by the PCM in the corners, and therefore to a practically negligible temperature variation. Focusing on the energy released by the metal parts of the storage tank and by the HTF, it can be observed that shorter storage periods meant lower energy released to the PCM, and of course, lower heat losses to the surroundings. Finally, despite observing a decrease of the PCM weighted average temperature during the storage process, the variation of PCM energy did not show the same tendency, but it showed an increase. This reflects the influence of the sensible region on the temperature behaviour while the energy variation was mainly influenced by the latent region.

When the RAE was increased (Figure 5b-5d and Table 5 to Table 7) some differences could be observed if compared to the process with a RAE 58% (Figure 5a). For the RAE 73% and the RAE 83%, a higher decrease of temperatures in the PCM located at the main and central regions and a higher increase of temperature in the PCM located in the corners was observed. However, it can be seen that at RAE 73% there was a change of tendency, and from this point on, the increase of temperature of the PCM located in the corners starts to be lower due to the increase of heat losses. Identically to temperatures, the PCM energy level showed a decrease in the main

and central regions and an increase in the corners. Moreover, there was a lower heat transfer from the HTF and metal parts of the storage tank to the PCM due to the fact that there were lower temperature gradients between the PCM and these two components. Finally, the behaviour of the TES system during the storage period which was previously fully charged (RAE 97%) deserves a separate mention. Notice that at the beginning of the storage process, there was an almost homogeneous temperature of the PCM at the inlet HTF temperature. The PCM temperature remained practically at the same homogeneous temperature during the whole period, with a temperature variation of 1.6 ºC after 120 min of storage. The high homogenization existing within the storage tank caused that the variation on the energy level was mainly due to heat losses.

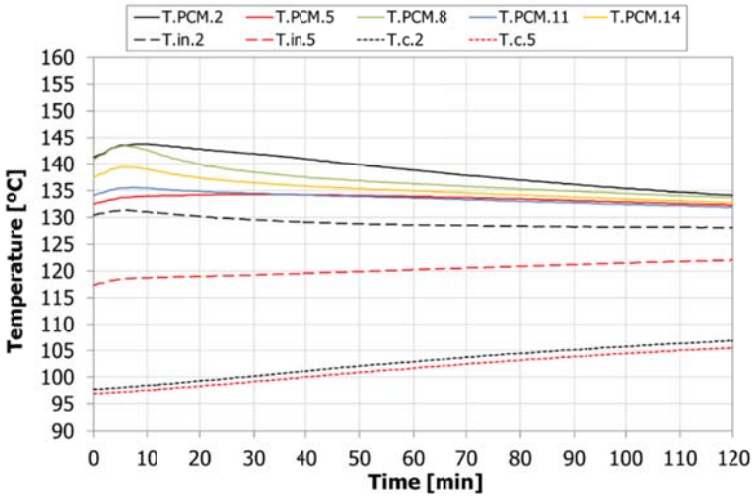

(a)

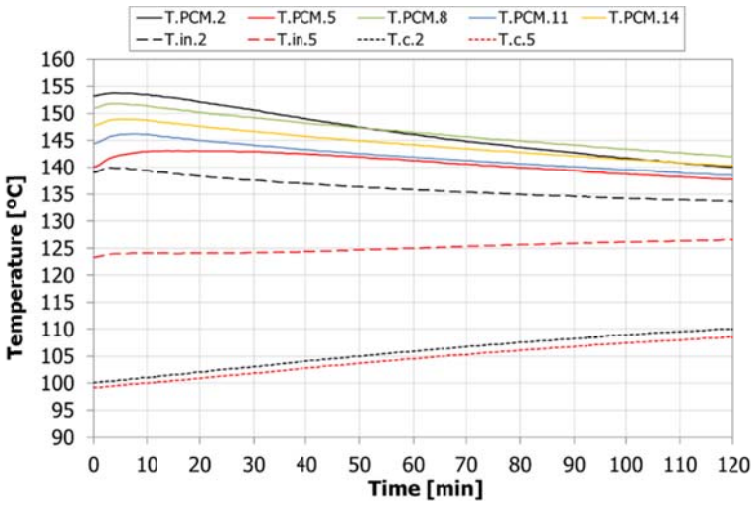

(b)

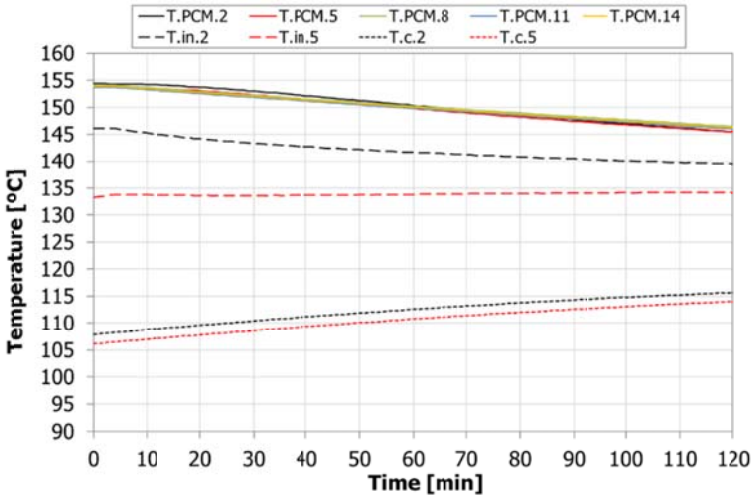

(c)

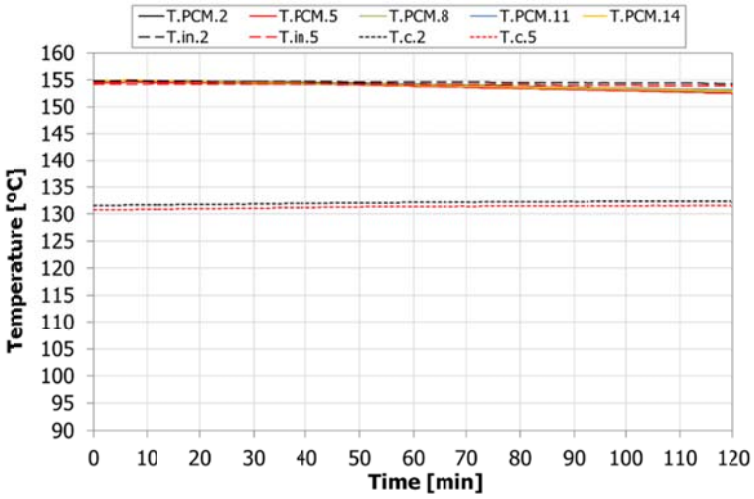

(d)

Figure 5. PCM temperature evolution during a storage period of 120 min: (a) RAE 58%; (b) RAE 73%; (c) RAE 83%; (d) RAE 97%. Due to the repeatability of the methodology and the experimental results, the evolution of the PCM temperature during the storage periods of 60 min and 25 min can be also observed in the same figures.

Table 4. Summary of the most important results during the storage process for a RAE 58%.

Parameter*		**Units**	**Storage period (Δt_{ST})**		
			25 min	**60 min**	**120 min**
Temperature variation of the whole PCM	$\Delta T_{PCM.total}$	[ºC]	- 0.33 (- 0.3%)	- 0.22 (- 0.2%)	- 2.95 (- 2.3%)
Temperature variation of the PCM located in the main region	ΔT_{PCM}	[ºC]	- 0.83 (- 0.6%)	- 0.78 (- 0.6%)	- 5.45 (- 4.0%)
Temperature variation of the PCM located in the central region	ΔT_{IN}	[ºC]	- 0.09 (- 0.1%)	+ 0.86 (+ 0.7%)	+ 0.41 (+ 0.3%)
Temperature variation of the PCM located in the corners	ΔT_{C}	[ºC]	+ 2.28 (+ 2.4%)	+ 2.35 (+ 2.4%)	+ 9.09 (+ 9.5%)
Energy variation of the whole PCM	$\Delta E_{PCM.total}$	[kWh]	+ 0.156 (+ 2.2%)	+ 0.049 (+ 0.7%)	- 0.250 (- 3.6%)
Energy variation of the PCM located in the main region	ΔE_{PCM}	[kWh]	+ 0.275 (+ 4.4%)	+ 0.079 (+ 1.3%)	- 0.240 (- 3.8%)
Energy variation of the PCM located in the central region	ΔE_{IN}	[kWh]	- 0.130 (- 17.3%)	- 0.059 (- 9.1%)	- 0.062 (- 9.4%)
Energy variation of the PCM located in the corners	ΔE_{C}	[kWh]	+ 0.012 (+36.3%)	+ 0.029 (+89.9%)	+ 0.052 (+ 164.2%)
Energy variation of the HTF	ΔE_{HTF}	[kWh]	- 0.070 (- 6.0%)	- 0.138 (- 11.7%)	- 0.182 (- 15.4%)
Energy variation of the metal parts of the storage tank	ΔE_{tank}	[kWh]	- 0.083 (- 2.4%)	- 0.187 (- 5.4%)	- 0.262 (- 7.5%)
Energy variation of the insulation	ΔE_{ins}	[kWh]	+ 0.084 (+ 3.6%)	+ 0.124 (+ 5.3%)	+ 0.200 (+ 8.4%)
Heat losses	ΔE_{loss}	[kWh]	- 0.087 (- 0.6%)	+ 0.152 (+ 1.1%)	+ 0.493 (+ 3.5%)

*The percentage between parentheses shows the percentage variation during the storage process compared to the value at the end of the charging process.

Table 5. Summary of the most important results during the storage process for a RAE 73%.

Parameter		**Units**	**Storage period (Δt_{ST})**		
			25 min	**60 min**	**120 min**
Temperature variation of the whole PCM	$\Delta T_{PCM.total}$	[ºC]	- 0.52 (- 0.4%)	- 2.99 (- 2.2%)	- 4.97 (- 3.7%)
Temperature variation of the PCM located in the main region	ΔT_{PCM}	[ºC]	- 1.00 (- 0.7%)	- 4.67 (- 3.3%)	- 7.85 (- 5.5%)
Temperature variation of the PCM located in the central region	ΔT_{IN}	[ºC]	- 0.71 (- 0.5%)	- 1.99 (- 1.5%)	- 2.52 (- 1.9%)
Temperature variation of the PCM located in the corners	ΔT_{C}	[ºC]	+ 2.18 (+ 2.2%)	+ 5.73 (+ 5.8%)	+9.56 (+ 9.7%)
Energy variation of the whole PCM	$\Delta E_{PCM.total}$	[kWh]	+ 0.071 (+ 0.8%)	- 0.160 (- 1.9%)	- 0.339 (- 4.0%)
Energy variation of the PCM located in the main region	ΔE_{PCM}	[kWh]	+ 0.062 (+ 0.8%)	- 0.176 (- 2.3%)	- 0.391 (- 5.2%)
Energy variation of the PCM located in the central region	ΔE_{IN}	[kWh]	- 0.004 (- 0.4%)	- 0.017 (- 1.7%)	- 0.005 (- 0.5%)
Energy variation of the PCM located in the corners	ΔE_{C}	[kWh]	+ 0.014 (+ 28.9%)	+ 0.033 (+ 71.5%)	+ 0.058 (+ 127.4%)
Energy variation of the HTF	ΔE_{HTF}	[kWh]	- 0.093 (- 7.7%)	- 0.113 (- 9.4%)	- 0.172 (- 14.2%)
Energy variation of the metal parts of the storage tank	ΔE_{tank}	[kWh]	- 0.137 (- 3.8%)	- 0.162 (- 4.5%)	- 0.267 (- 7.4%)
Energy variation of the insulation	ΔE_{ins}	[kWh]	+ 0.073 (+ 3.2%)	+ 0.121 (+ 4.8%)	+ 0.182 (+ 7.2%)
Heat losses	ΔE_{loss}	[kWh]	+ 0.086 (+ 0.5%)	+ 0.314 (+ 2.0%)	+ 0.596 (+ 3.8%)

Table 6. Summary of the most important results during the storage process for a RAE 83%.

Parameter		Units	Storage period (Δt_{ST})		
			25 min	**60 min**	**120 min**
Temperature variation of the whole PCM	$\Delta T_{PCM.total}$	[ºC]	- 1.14 (- 0.8%)	- 3.43 (- 2.4%)	- 5.41 (- 3.8%)
Temperature variation of the PCM located in the main region	ΔT_{PCM}	[ºC]	- 1.60 (- 1.1%)	- 4.81 (- 3.2%)	- 7.78 (- 5.2%)
Temperature variation of the PCM located in the central region	ΔT_{IN}	[ºC]	- 2.27 (- 2.4%)	- 4.14 (- 2.9%)	-5.10 (- 3.6%)
Temperature variation of the PCM located in the corners	ΔT_{C}	[ºC]	+ 1.97 (+ 1.8%)	+ 4.45 (+ 4.2%)	+ 7.41 (+ 7.0%)
Energy variation of the whole PCM	$\Delta E_{PCM.total}$	[kWh]	- 0.107 (- 1.1%)	- 0.270 (- 2.8%)	- 0.394 (- 4.1%)
Energy variation of the PCM located in the main region	ΔE_{PCM}	[kWh]	- 0.080 (- 1.0%)	- 0.260 (- 3.2%)	- 0.437 (- 5.4%)
Energy variation of the PCM located in the central region	ΔE_{IN}	[kWh]	- 0.040 (- 2.8%)	- 0.038 (- 2.7%)	- 0.008 (- 0.6%)
Energy variation of the PCM located in the corners	ΔE_{C}	[kWh]	+ 0.013 (+ 13.7%)	+ 0.029 (+ 32.0%)	+ 0.051 (+ 56.7%)
Energy variation of the HTF	ΔE_{HTF}	[kWh]	- 0.039 (- 3.2%)	- 0.073 (- 6.0%)	- 0.118 (- 9.8%)
Energy variation of the metal parts of the storage tank	ΔE_{tank}	[kWh]	- 0.057 (- 1.5%)	- 0.127 (- 3.4%)	- 0.195 (- 5.3%)
Energy variation of the insulation	ΔE_{ins}	[kWh]	+ 0.050 (+ 2.0%)	+ 0.054 (+ 2.0%)	+ 0.120 (+ 4.5%)
Heat losses	ΔE_{loss}	[kWh]	+ 0.152 (+ 0.9%)	+ 0.415 (+ 2.4%)	+ 0.588 (+ 3.4%)

Table 7. Summary of the most important results during the storage process for a RAE 97%.

Parameter		Units	Storage period (Δt_{ST})		
			25 min	**60 min**	**120 min**
Temperature variation of the whole PCM	$\Delta T_{PCM.total}$	[ºC]	- 0.06 (- 0.0%)	- 0.75 (- 0.5%)	- 1.60 (- 1.1%)
Temperature variation of the PCM located in the main region	ΔT_{PCM}	[ºC]	- 0.09 (- 0.1%)	-0.97 (- 0.6%)	- 2.05 (- 1.3%)
Temperature variation of the PCM located in the central region	ΔT_{IN}	[ºC]	- 0.09 (- 0.1%)	- 0.40 (- 0.3%)	- 0.90 (- 0.6%)
Temperature variation of the PCM located in the corners	ΔT_{C}	[ºC]	+ 0.17 (+ 0.1%)	+ 0.24 (+ 0.2%)	+ 0.57 (+ 0.4%)
Energy variation of the whole PCM	$\Delta E_{PCM.total}$	[kWh]	- 0.013 (- 0.1%)	- 0.048 (- 0.4%)	- 0.095 (- 0.9%)
Energy variation of the PCM located in the main region	ΔE_{PCM}	[kWh]	- 0.016 (- 0.2%)	- 0.054 (- 0.6%)	- 0.124 (- 1.4%)
Energy variation of the PCM located in the central region	ΔE_{IN}	[kWh]	- 0.002 (- 0.1%)	- 0.004 (- 0.2%)	- 0.010 (- 0.6%)
Energy variation of the PCM located in the corners	ΔE_{C}	[kWh]	+ 0.005 (+ 1.0%)	+ 0.010 (+ 2.2%)	+ 0.039 (+ 8.7%)
Energy variation of the HTF	ΔE_{HTF}	[kWh]	- 0.016 (- 1.3%)	- 0.027 (- 2.3%)	- 0.043 (- 3.6%)
Energy variation of the metal parts of the storage tank	ΔE_{tank}	[kWh]	- 0.031 (- 0.8%)	- 0.057 (- 1.5%)	- 0.099 (- 2.5%)
Energy variation of the insulation	ΔE_{ins}	[kWh]	- 0.009 (- 0.3%)	- 0.024 (- 0.8%)	- 0.032 (- 1.0%)
Heat losses	ΔE_{loss}	[kWh]	+ 0.069 (+ 0.4%)	+ 0.156 (+ 0.8%)	+ 0.270 (+ 1.4%)

3.3 Discharging process

The influence of the storage period on the discharge process was evaluated from thermal and heat transfer rates points of view. Figure 6 shows the temperature evolution of the weighted average temperature of the PCM located in the three characteristic regions of the storage tank (Figure 2b), during the first 180 min of discharge. The first thing it can be observed is that the temperature profiles showed higher values when the previous charging processes were performed at higher RAE. This picture was the same in all three regions of the storage tank and independently of the storage period duration. The second thing that can be observed is that slight variations could be observed on the temperature profiles when the RAE was kept constant and only the storage period was modified. However, the influence of the storage period length is analysed in each region of the storage tank separately. If considering PCM located in the main region (Figure 6a), it can be seen that the discharging processes which were preceded by short storage periods (no matter which RAE was) presented higher average temperature values until one point (i.e: t=40 min in RAE 58% or t=80 min in RAE 73%), where this tendency is reversed. The instant where the change of tendency took place depended on the RAE of the previous charging period, being faster for lower RAE. The PCM located in the central region (Figure 6b) showed a similar temperature evolution than the previous case, but with slightly lower average values. However, the change of tendency depending on the storage period took place earlier in all cases. The higher homogenisation of temperatures existing in the latent TES system after a larger storage period causes its average temperature to reach faster the temperature of the HTF. The PCM located in the corners (Figure 6c) showed a behaviour totally different than the PCM located in the previous two regions. The first difference was that the temperature of the processes which were preceded by longer storage periods was higher, as observed in section 3.2. The second difference was that, due to their location far from the tubes bundle and the low thermal conductivity of the PCM, the discharge of energy is penalized in this region and its average temperature keeps increasing until one point, where the combination of heat losses and low temperature of the HTF cause the average PCM temperature to start decreasing. The high temperature homogenisation existing in the storage tank at the beginning of the discharging processes preceded by full charging processes (RAE 97%), which caused that there was no increase of temperatures at any moment of the process and that after 40 min, the temperatures started to decrease for the same reasoning than before.

Figure 7 shows the evolution of the HTF heat transfer rate during the discharging processes for different storage periods (Δt_{ST}=25 min, 60 min, and 120 min) and preceded by charging processes at different energy levels (RAE 58%, RAE 73%, RAE 83%, and RAE 97%). Similar to the temperature profiles evolution, the length of the storage period slightly affected heat

transfer rates during the discharging process. As expected, higher heat transfer rate values were observed when the charging level of the preceding processes was higher. Focusing on such energy levels, it can be observed that when the TES system was partially charged at a RAE 58% (Figure 7a), the fact of extending the storage period from 25 min to 60 min and 120 min, caused differences in the average heat transfer values during the first 30 min of discharge between 3.6% and 9.9%, respectively. After that moment, the heat transfer profiles in all cases practically showed the same behaviour. When the TES system was partially charged at a RAE 73% (Figure 7b), the first 30 min of the discharging processes which were preceded by storage periods of 60 min and 120 showed differences up to 15.9% and 17.2%, respectively, if compared to the process preceded by a storage period of 25 min. The heat transfer rates of discharging processes which followed a process of partial charge at a RAE 83% (Figure 7c) showed small differences when the storage period lasted 60 min (3.7% if compared to a storage period of 25 min) but it significantly increased to 9.5% when the storage period was extended to 120 min. Finally, the high homogenisation existing after a full charging process (Figure 7d) caused that the influence of the storage period was practically null in the heat transfer rate profiles, observing differences of 2.5% between the process preceded by a 120-min storage period and the process preceded by a 60-min storage period during the first 30 min of discharge.

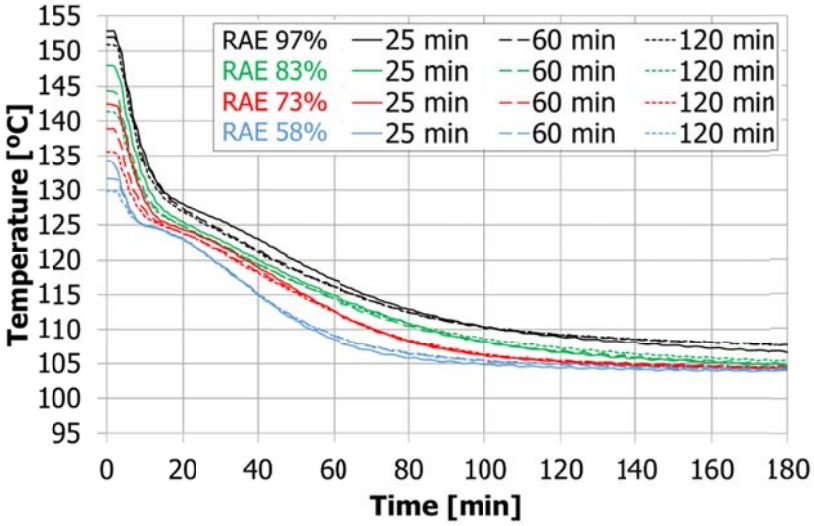

(a)

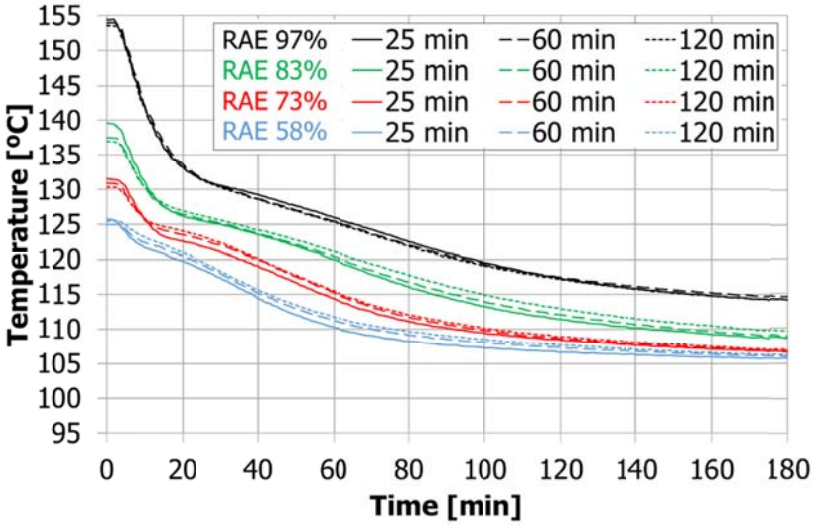

(b)

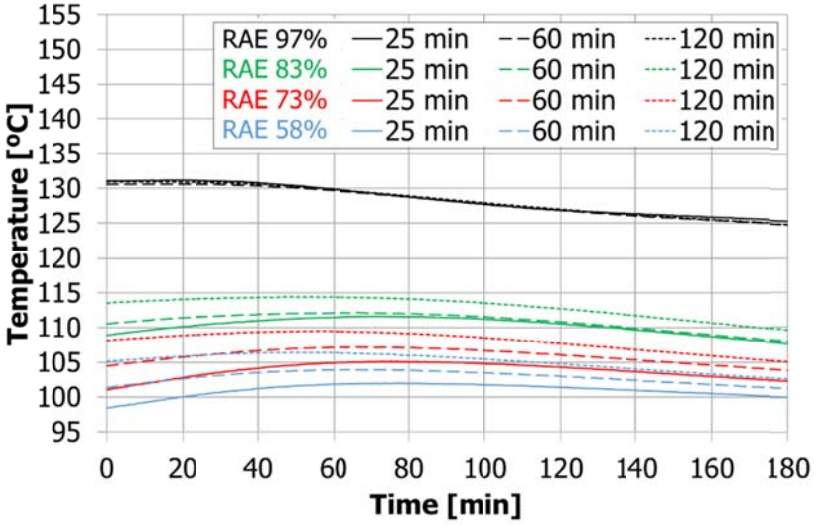

(c)

Figure 6. Evolution, during the discharge, of the weighted average temperature of the PCM located in the main region (a), in the central region (b), and in the corners (c) for different periods of storage: 25 min, 60 min, and 120 min

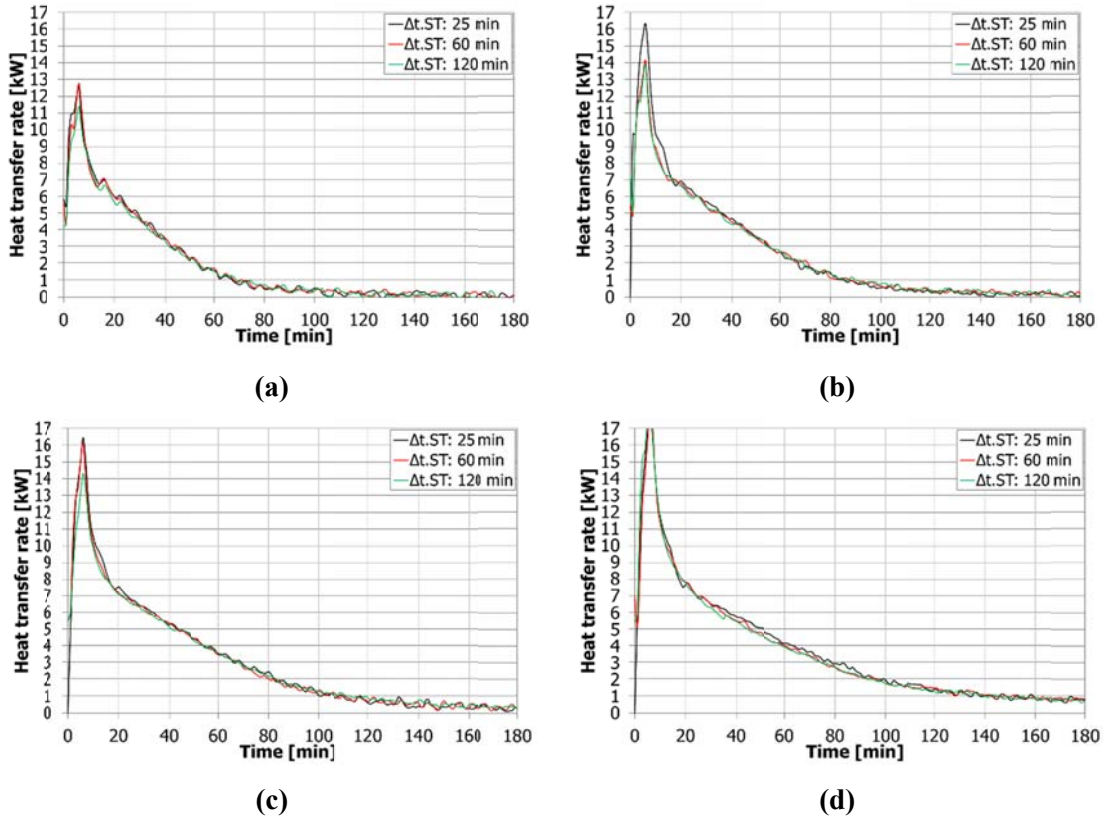

Figure 7. Evolution of the HTF heat transfer rate during the discharging processes for different storage periods (Δt_{ST}=25 min, 60 min, and 120 min) and preceded by charging processes at different energy levels: (a) RAE 58%; (b) RAE 73%; (c) RAE 83%; (d) RAE 97%.

3.4 Uncertainty analysis results

To get an insight on the importance of the uncertainties in the results presented in this study, Table 8 shows the results of the uncertainty analysis calculated for the case in which the tank was charged up to RAE 83%, and the storage period was 60 minutes. This case was selected since the authors considered it could give more representative values. The values of the HTF power uncertainty refer to the average value of $\dot{Q}_{HTF,dch}$ over the first 30 minutes of discharge.

Table 8. Summary of the uncertainty analysis results, for a RAE 83% and a storage period of 60 minutes.

Parameter		Units	Value*
Temperature variation of the whole PCM	$\Delta T_{PCM.total}$	[ºC]	± 0.05 (± 1.5%)
Temperature variation of the PCM located in the main region	ΔT_{PCM}	[ºC]	± 0.07 (± 1.4%)
Temperature variation of the PCM located in the central region	ΔT_{IN}	[ºC]	± 0.10 (± 2.4%)
Temperature variation of the PCM located in the corners	ΔT_{C}	[ºC]	± 0.10 (+ 2.3%)
Energy variation of the whole PCM	$\Delta E_{PCM.total}$	[kWh]	± 0.028 (± 10.2%)
Energy variation of the PCM located in the main region	ΔE_{PCM}	[kWh]	± 0.026 (± 10.1%)
Energy variation of the PCM located in the central region	ΔE_{IN}	[kWh]	± 0.008 (± 20.6%)
Energy variation of the PCM located in the corners	ΔE_{C}	[kWh]	± 0.004 (± 13.3%)
Energy variation of the HTF	ΔE_{HTF}	[kWh]	± 0.004 (± 5.5%)
Energy variation of the metal parts of the storage tank	ΔE_{tank}	[kWh]	± 0.013 (± 10.0%)
Energy variation of the insulation	ΔE_{ins}	[kWh]	± 0.038 (± 70.2%)
Heat losses	ΔE_{loss}	[kWh]	± 0.049 (± 11.8%)
HTF heat transfer rate	$\dot{Q}_{HTF,dch}$	[kW]	± 0.54 (± 6.1%)

* The percentage between parentheses shows the relative uncertainty in relation to the value of the parameter during the process.

Table 6 shows that the errors associated to the PCM temperature measurements are small compared to the PCM temperature variations in the different regions of the tank. The errors associated to the variations of the energy stored in the PCM are relatively high, but still much lower than the corresponding variations during the storage period. The highest relative uncertainty of the PCM energy variations corresponds to the central part of the tank ($\Delta E_{PCM.in}$). The uncertainty of the energy variations of the HTF are in between the uncertainties of the PCM temperature and PCM energy, while the uncertainties of the metal parts of the storage tank and of the heat losses are comparable to that of the PCM energy. The only variable that has a relatively high uncertainty is the variation of the energy stored in the insulation. Thus, one has to pay more attention to the correct quantification of this variable. Finally, the uncertainty associated to the average HTF power during the first 30 minutes of discharge is also relatively low; nevertheless, they are comparable with the results obtained regarding the variation of the average HTF power with respect to the case in which the storage period was 25 minutes.

4 Conclusions

The experimental research presented in this paper aims at studying the influence of the duration of the storage period in a latent heat TES system which was partially charged on its subsequent discharging process. Three different storage periods were evaluated (25 min, 60 min, and 120 min), which followed charging processes which were charged at different energy levels (58%, 73%, 83% (partial charge), and 97% (full charge)).

Results showed that during the storage periods which followed partially charged processes there was an energy homogenization process not only as a result of the temperature gradients existing within the different regions of the storage tank, but also as a result of the heat losses to the surroundings. When the storage period was increased, higher energy transference from the main region to the corners was observed. Due to the geometry of the TES system, it was desired that the energy was contained in the main region rather than in the corners, where the energy is more difficult to recover from. Moreover, heat losses were also increased no matter the value of the RAE. Therefore, the length of the storage period which follows an incomplete charge has an influence on the modification of the discharging process initial map. This is important for numerical models, since they usually consider at the beginning of the discharge the same map than the existing at the end of the charge.

During the discharging process, it was observed that the length of the storage period had a higher influence when the RAE was intermediate (RAE 73%), and not that important for lower (RAE 58%) or higher values (RAE 97%). However, it can be stated that this effect is not very significant, and it only can be observed during the first 30 min of discharge as a result of the temperature at which the discharging process starts.

Acknowledgements

This work was partially funded by the Ministerio de Economía y Competitividad de España (ENE2015-64117-C5-1-R (MINECO/FEDER) and ENE2015-64117-C5-3-R (MINECO/FEDER)). The authors would like to thank the Catalan Government for the quality accreditation given to their research group (2017 SGR 1537). GREA is certified agent TECNIO in the category of technology developers from the Government of Catalonia. Jaume Gasia would like to thank the Departament d'Universitats, Recerca i Societat de la Informació de la Generalitat de Catalunya for his research fellowship (2018 FI_B2 00100).

References

1. A. Gil, M. Medrano, I. Martorell, A. Lázaro, P. Dolado, B. Zalba, L.F. Cabeza, State of the art on high temperature thermal energy storage for power generation. Part 1—Concepts, materials and modellization, Renewable and Sustainable Energy Reviews 14(1) (2010) 31-55.
2. S. Brückner, S. Liu, L. Miró, M. Radspieler, L.F. Cabeza, E. Lävemann, Industrial waste heat recovery technologies: An economic analysis of heat transformation technologies, Applied Energy 151 (2015) 157-167.
3. I. Dincer, M.A. Rosen, Thermal energy storage: systems and applications, Second edition., Chichester: John Wiley & Sons (2010). ISBN: 978-0-470-74706-3.
4. H. Mehling, LF. Cabeza, Heat and cold storage with PCM. An up to date introduction into basics and applications. Berlin, Germany. Springer-Verlag 2008. ISBN: 979-3-540-68556-2.
5. D. Macphee, I. Dincer, Performance assessment of some ice TES systems, International Journal of Thermal Sciences 48 (2009) 2288–2299.
6. G. Li, Energy and exergy performance assessments for latent heat thermal energy storage systems, Renewable and Sustainable Energy Reviews 51 (2015) 926–954.
7. H. El-Dessouky, F. Al-Juwayhel, Effectiveness of a thermal energy storage system using phase-change materials, Energy Conversion and Management 38(6) (1997) 601-617.
8. F. Agyenim, P. Eames, M. Smyth, Heat transfer enhancement in medium temperature thermal energy storage system using a multitube heat transfer array, Renewable Energy 35(1) (2010) 198-207.
9. L. Li, H. Yu, X. Wang, S. Zheng. Thermal analysis of melting and freezing processes of phase change materials (PCMs) based on dynamic DSC test. Energy and Buildings 130 (2016) 388–396.
10. M. Toksoy, Z. Ilken, The effects of phase change during the stand-by period in latent heat energy storage systems, Solar Energy 47(2) (1991) 69-73.
11. G. Bejarano, J.J. Suffo, M. Vargas, M.G. Ortega, Novel scheme for a PCM-based cold energy storage system. Design, modelling, and simulation, Applied Thermal Engineering 132 (2018) 256–274.
12. S. Jegadheeswaran, S.D. Pohekar, T. Kousksou, Exergy based performance evaluation of latent heat thermal storage system: A review, Renewable and Sustainable Energy Reviews 14 (2010) 2580–2595.
13. S. Hirano, Performance of supercooled thermal energy storage unit. 1st International Energy Conversion Engineering Conference, USA (2003).

14. H. Singh, R.P. Saini, J.S. Saini, A review on packed bed solar energy storage systems, Renewable and Sustainable Energy Reviews 14(3) (2010) 1059-1069.
15. Y.M. Han, R.Z. Wang, Y.J. Dai, Thermal stratification within the water tank, Renewable and Sustainable Energy Reviews 13(5) (2009) 1014-1026.
16. C. Prieto, L. Miró, G. Peiró, E. Oró, A. Gil, L.F. Cabeza, Temperature distribution and heat losses in molten salts tanks for CSP plants, Solar Energy 135 (2016) 518-526.
17. F. Kuznik, J. Virgone, Experimental investigation of wallboard containing phase change material: Data for validation of numerical modelling, Energy and Buildings 41 (2009) 561–570.
18. X. Jin, H. Hu, X. Shi, X. Zhang, Energy asymmetry in melting and solidifying processes of PCM, Energy Conversion and Management 106 (2015) 608–614.
19. Bony, S. Citherlet, Numerical model and experimental validation of heat storage with phase change materials, Energy Buildings 39 (2007) 1065–1072.
20. J. Rose, A. Lahme, N.U. Christensen, P. Heiselberg, M. Hansen, K. Grau. Numerical method for calculating latent heat storage in constructions containing phase change material. In Proceedings of Building Simulation 2009: 11th Conference of the International Building Performance Simulation Association, 400–407. Glasgow, Scotland, GBR, July 27–30.
21. R. Chandrasekharan, E.S. Lee, D.E. Fisher, P.S. Deokar. An enhanced simulation model for building envelopes with phase change materials, ASHRAE Trans, 119 (2013).
22. B. Delcroix. Modelling of Thermal Mass Energy Storage in Buildings with Phase Change Materials. PhD dissertation, Department of Mechanical Engineering, École Polytechnique de Montréal, Montréal, QC, Canada (2015).
23. L. Li, H. Yu, X. Wang, S. Zheng. Thermal analysis of melting and freezing processes of phase change materials (PCMs) based on dynamic DSC test. Energy and Buildings 130 (2016) 388–396.
24. J.P. Bédécarrats, J. Castaing-Lasvignottes, F. Strub, J.P. Dumas. Study of a phase change energy storage using spherical capsules. Part I: Experimental results. Energy Conversion and Management 50 (2009) 2527–2536.
25. K. D'Avignon, M. Kummert. Experimental assessment of a phase change material storage tank. Applied Thermal Engineering 99 (2016) 880–891.
26. V. Palomba, V. Brancato, A. Frazzica. Experimental investigation of a latent heat storage for solar cooling applications Applied Energy 199 (2017) 347-358.
27. J. Gasia, A. de Gracia, G. Peiró, S. Arena, G. Cau, L.F. Cabeza, Use of partial load operating conditions for latent thermal energy storage management, Applied Energy 216 (2018) 234-242.

28. C. Zauner, F. Hengstberger, M. Etzel, D. Lager, R. Hofmann, H. Walter, Experimental characterization and simulation of a fin-tube latent heat storage using high density polyethylene as PCM, Applied Energy 179 (2016) 237-246.
29. C. Yang, M.E. Navarro, B. Zhao, G. Leng, G. Xu, L. Wang, Y. Jin, Y. Ding. Thermal conductivity enhancement of recycled high density polyethylene as a storage media for latent heat thermal energy storage, Solar Energy Materials and Solar Cells 152 (2016) 103-110
30. Repsol Alcudia 6020L Data sheet. REPSOL Chemicals. < https://portalquimica.repsol.com/ccrz__CCPage?pageKey=detail&id=a1xb0000001GyjHAAS&cclcl=en_US> (last accessed on 05/01/2018).
31. C. Rathgeber, H. Schmit, L. Miró, L.F Cabeza, A. Gutierrez, S.N Ushak, S. Hiebler. Enthalpy-temperature plots to compare calorimetric measurements of phase change materials at different sample scales. Journal of Energy Storage 15 (2018) 32-38.
32. G. Peiró, C. Prieto, J. Gasia, A. Jové, L. Miró, L.F. Cabeza, Two-tank molten salts thermal energy storage system for solar power plants at pilot plant scale: lessons learnt and recommendations for its design, start-up and operation, Renewable energy 121 (2018) 236-248.
33. H. Benoit, D. Spreafico, D. Gauthier, G. Flamant, Review of heat transfer fluid in tube – receivers used in concentrating solar thermal systems: Properties and heat transfer coefficients, Renewable Sustainable Energy Reviews 55 (2016) 298–315.
34. J.P. Holman, Experimental Methods for Engineers, eight ed. McGrawHill, Newyork (2012).